

Available online at www.sciencedirect.com

SCIENCE @ DIRECT®

Inorganica Chimica Acta 357 (2004) 4078–4084

**Inorganica
Chimica Acta**www.elsevier.com/locate/ica

Synthesis, photophysical characterisation and metal ion binding properties of new ligands containing anthracene chromophores

Fabrizio Bolletta^a, Andrea Garelli^a, Marco Montalti^a, Luca Prodi^{a,*}, Silvia Romano^a,
Nelsi Zaccheroni^a, Luciano Canovese^b, Gavino Chessa^b, Claudio Santo^b,
Fabiano Visentin^b

^a *Dipartimento di Chimica, "G. Ciamician", Università degli studi di Bologna, Via Selmi 2, I 40126, Bologna, Italy*

^b *Dipartimento di Chimica, Università degli Studi di Venezia, Calle Larga S. Marta 2137, I 30123 Venezia, Italy*

Received 7 November 2003; accepted 1 May 2004

Available online 9 June 2004

Abstract

Two new fluorescent chemosensors for heavy metal ions have been synthesised and their photophysical properties have been investigated. They present a pyridyl-thioether-based binding site and the anthracene moiety as a chromophore. In the experimental conditions used, no evidence is found for the formation of complexes with Pb^{2+} , Zn^{2+} , Cd^{2+} , and Ag^{+} ions. On the contrary, in acetonitrile solutions both ligands strongly bind Cu^{2+} and Hg^{2+} cations according to a 1:1 and a 1:2 (metal:ligand) stoichiometry. In these complexes, the intense luminescence typical of anthracene derivatives is almost completely quenched and this phenomenon can be mainly attributed to an intraligand electron transfer process from the anthracene chromophore to the complexed pyridine. These results are of interest for the development of new chemosensors for the design of efficient electronic tongues for the detection of transition metal ions.

© 2004 Elsevier B.V. All rights reserved.

Keywords: Fluorescence; Chemosensor; Mercury; Copper; Anthracene

1. Introduction

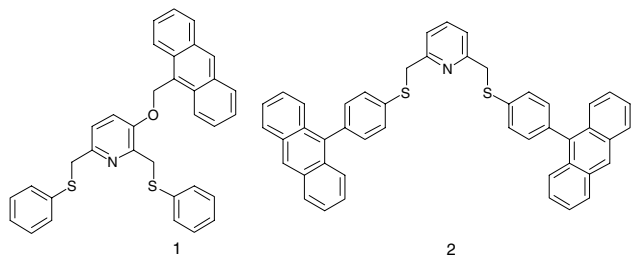
The preparation and characterisation of new chemosensors represents the first step for the development and fabrication of efficient devices for the real time determination of chemical species [1–8]. Of the various kinds of chemosensors, the luminescent ones present many advantages, since luminescence measurements are usually very sensitive, low cost, easily performed, and versatile [9]. Such devices find wide applications in many disciplines such as medical diagnostics, clinical and medical sciences, biochemistry, analytical chemistry and environmental science [6–8].

For this reason, many efforts are devoted to the design of more and more efficient chemosensors and, as a consequence, a huge number of papers have been recently published.

For the detection of the target analyte, two different processes are needed: molecular recognition and signal transduction, i.e., the mechanism by which the complexation of the sensor with the analyte causes a change in the properties of the sensor itself. Chemosensors present, therefore, components able to perform all these functions. In this manuscript, we report the synthesis, photophysical characterisation and metal ion binding properties of ligands **1** and **2**. These ligands possess an anthracene chromophore as signalling unit, and a chelating unit composed of two sulfur atoms and a pyridine, designed to coordinate transition metal ions.

* Corresponding author. Tel.: +390512099481; fax: +390512099456.

E-mail addresses: lprodi@unibo.it, luca.prodi@unibo.it (L. Prodi), chessa@unive.it (G. Chessa).



2. Experimental

2.1. Materials and general procedures

Tetrahydrofuran (THF) was distilled from Na benzophenone just before use. *N,N*-Dimethylformamide (DMF) was purified by distillation from CaH₂ and stored over 4 Å molecular sieves in a dark bottle.

The solvent used for photophysical measurements was acetonitrile from Merck (UVASOL). All other reagents were purchased from Fluka/Aldrich and used as such. All the metal ions were added as perchlorate salts.

2,6-Bis(phenylthiomethyl)-3-hydroxypyridine (**3**) [10] and 2,6-bis(chloromethyl)pyridine (**4**) [11] were prepared as described previously. ¹H NMR and ¹³C NMR spectra were recorded in deuteriochloroform on a Bruker 300 spectrometer at 300 and 75 MHz, respectively, using the solvent signal as internal standard.

GC–MS spectra were recorded on a Thermo Quest Finnigan Trace 2000 Series gas chromatograph–mass spectrometer using a Mega Fused Silica capillary column (stationary phase: SE52, 30 m × 0.25 mm i.d.). Flash chromatographic separations were performed by a Gyan JaiFlash apparatus equipped with a silica gel prepacked cartridge.

Electrospray ionisation mass spectra were obtained with Agilent Technologies MSD1100 single-quadrupole mass spectrometer. Mass spectra were acquired in scan positive ion mode from *m/z* 100 to *m/z* 2500, with a scan time of 0.1 s. The parameters of the spray chamber were set as follows: drying gas flow at 8 ml min⁻¹, nebulizer (nitrogen) pressure at 30 psi, the temperature at 350 °C, and the ESI spray voltage at 5000 V.

2.2. Synthesis of the ligands

2.2.1. 3-(9-Anthrylmethoxy)-2,6-bis(phenylthiomethyl)pyridine (**1**)

A mixture of 2,6-bis(phenylthiomethyl)-3-hydroxypyridine (**3**) (1.02 g, 3 mmol) and anhydrous K₂CO₃ (0.49 g, 3.6 mmol) in dry DMF (10 ml) was stirred under reduced pressure at room temperature for 30 min, after which 9-chloromethylantracene (0.75 g, 3.3 mmol) was added and the reaction mixture was heated at 65 °C for

24 h under an argon atmosphere. The mixture was evaporated to dryness and the residue was partitioned between dichloromethane and water. The organic extract was washed with water, dried with Na₂SO₄, and evaporated to give yellow solid. The crude product was purified by flash chromatography eluting sequentially with dichloromethane–hexane (7:3), dichloromethane–hexane (85:15), and dichloromethane to give **1** as a pale yellow solid (1.33 g, 84% yield), m.p. 102–105 °C. *Anal.* Calc. for C₃₄H₂₇NOS₂: C, 77.09; H, 5.14; N, 2.64. Found: C, 77.32; H, 4.98; N, 2.81%. ¹H NMR: δ 4.18 (2H, s, CH₂S), 4.27 (2H, s, CH₂S), 5.97 (2H, s, CH₂O), 6.98–7.59 (m, 16H, 3,4-PyrH and ArH), 8.08 (2H, m, ArH), 8.29 (2H, m, ArH), and 8.57 (1H, s, ArH). ¹³C NMR: δ 35.9 (CH₂S), 39.8 (CH₂S), 64.0 (CH₂O), 122.7 (5-PyC), 124.3 (4-PyC), 125.6, 126.2, 126.4, 126.6, 127.1, 128.8, 129.3, 129.5, 129.6, 129.7, 129.9, 131.4, 131.8, 136.8, 137.2, 148.1 (2-PyC), 149.1 (6-PyC) and 152.4 (3-PyC). ESI-MS: *m/z* 530 [M + H]⁺, 552 [M + Na]⁺, 568 [M + K]⁺, 1081 [2M + Na]⁺.

2.2.2. 4-(*tert*-Butylthio)phenylboronic acid (**6**)

n-Butyllithium (1.6 M solution in hexane, 48 ml, 77 mmol) was slowly added to a stirred solution of 4-(*tert*-butylsulfanyl)bromobenzene (**5**) (11.78 g, 48 mmol) in dry THF (40 ml) cooled at –78 °C and under an argon atmosphere. After 20 min triisopropyl borate (58 ml, 250 mmol) was added and the resulting mixture was maintained at –78 °C for two hours, then allowed to warm to room temperature and stirred overnight. After addition of water (50 ml), the reaction mixture was evaporated under reduced pressure to remove the organic solvent. The resulting aqueous phase was extracted with diethylether and the combined organic extracts were washed with water, dried with Na₂SO₄, and finally evaporated to dryness. The crude product was recrystallised from diethylether–hexane to give **6** as a white solid (8.75 g, 87%), m.p. 168–170 °C. *Anal.* Calc. for C₁₀H₁₅BO₂S: C, 57.17; H, 7.20. Found: C, 57.38; H, 7.15%. ¹H NMR (CDCl₃): 1.37 (9H, s, C(CH₂)₃), 7.70 (2H, d, *J* 8.1, 2,6-ArH), and 8.20 (2H, d, *J* 8.1, 3,5-ArH). ¹³C NMR (CDCl₃): δ 31.5 C(CH₃)₃, 47.0 C(CH₃)₃, 135.9 (3,5-ArC), 137.0 (2,6-ArC), and 138.8 (4-ArC).

2.2.3. 9-[4-(*tert*-Butylthio)phenyl]anthracene (**7**)

To a mixture of benzene (120 ml), EtOH (20 ml), and water (40 ml) were added 9-bromoanthracene (5.14 g, 20 mmol), 4-(*tert*-butylsulfanyl)phenylboronic acid (**6**) (5.46 g, 26 mmol), (PPh₃)₄Pd (0.69 g, 0.6 mmol), and K₂CO₃ (11.06 g, 80 mmol). The reaction mixture was refluxed under an argon atmosphere for 24 h and, after cooling to room temperature, benzene (50 ml) was added. The organic layer was washed with brine, dried with Na₂SO₄, and evaporated to dryness. The crude product was purified by flash chromatography eluting

sequentially with hexane–dichloromethane mixtures (95:5 and 90:10) to give **7** as a pale green-yellow crystalline solid (6.3 g, 92%), m.p. 119–121 °C. *Anal. Calc.* C₂₄H₂₂S: C, 84.16; H, 6.47. Found: C, 83.30; H, 6.34%. ¹H NMR (CDCl₃): δ 1.46 (9H, s, C(CH₂)₃), 7.37–7.52 (6H, m, ArH), 7.66 (2H, d, *J* 8.6, ArH), 7.77 (2H, d, *J* 7.9, ArH), 8.07 (2H, d, *J* 8.3, ArH), and 8.53 (1H, s, ArH). ¹³C NMR (CDCl₃): δ 31.6 C(CH₃)₃, 46.5 C(CH₃)₃, 125.6, 125.9, 127.0, 127.2, 128.8, 130.5, 131.7, 131.8, 132.4, 136.6, 137.7, and 139.7. MS (*m/z*, %): 342 (72), 286 (100), 252 (86), 239 (20), 226 (14), 213 (6), 202 (5), 113 (5), 57 (84), and 41 (50).

2.2.4. 9-(4-Mercaptophenyl)-anthracene (**8**)

To a solution of *tert*-butyl protected thiol **7** (2.23 g, 6.5 mmol) in thioanisole (20 ml) at 0 °C were added TFA (2.52 g, 22.1 mmol) and trifluoromethanesulfonic acid (1.95 g, 13 mmol). The reaction mixture was allowed to react 1 h at room temperature then, after cooling to 0 °C, water (10 ml) was added and the resulting mixture was neutralised with NaOH 2 M and extracted with dichloromethane. The organic extract was washed with water, dried with Na₂SO₄, and distilled under reduced pressure to afford the crude product, which was recrystallised from dichloromethane–hexane to yield **8** as a pale yellow solid (1.57 g, 84%).

This sample showed by ¹H NMR and GC–MS analysis to contain a small amount (<5%) of 9-[4-(methylsulfanyl)phenyl]anthracene. Thus, it was chromatographed on silica gel eluting sequentially with hexane and hexane–dichloromethane mixtures (95:5 and 90:10). Unfortunately, the sample was recovered unchanged. ¹H NMR (CDCl₃): δ 2.64 (0.15H, s, CH₃), 3.63 (1H, s, SH), 7.30–7.44 (4H, m, ArH), 7.44–7.54 (4H, m, ArH), 7.68 (2H, d, *J* 8.7, ArH), 8.06 (2H, d, *J* 8.5, ArH), and 8.51 (1H, s, ArH). ¹³C NMR (CDCl₃): δ 16.2 (CH₃), 125.5, 125.8, 127.0, 127.1, 128.8, 129.8, 130.4, 130.6, 131.8, 132.4, 136.4, and 136.6. MS (*m/z*, %): 286 (100), 252 (85), 239 (12), 226 (12), 213 (5), 202 (5), 143 (8), 126 (90), and 113 (41).

2.2.5. 2,6-Bis-(4-anthracen-9-yl-phenylthiomethyl)-pyridine (**2**)

A solution of thiol **8** (1.03 g, 3.6 mmol) in dry THF (50 ml) containing NaH (0.29 g, 7.2 mmol) was stirred for 1 h under an argon atmosphere, then dichloride **4** (0.26 g, 1.5 mmol) was added and the resulting mixture was heated at 40 °C for 24 h. After removal of the solvent, the residue was partitioned between ethyl acetate and water. The organic phase was washed with NaOH 2 M, brine, then dried with Na₂SO₄ and evaporated to dryness. The residue was chromatographed on silica gel eluting sequentially with hexane–dichloromethane mixtures (1:1 and 3:7) to give **2** as a pale yellow solid (0.875g, 86%), m.p. 193–194 °C. *Anal. Calc.* for

C₄₇H₃₃NS₂: C, 83.52; H, 4.92; N, 2.07. Found: C, 82.64; H, 4.86, N, 2.07%. ¹H NMR (CDCl₃): δ 4.43 (4H, s, CH₂), 7.30–7.33 (8H, m, ArH), 7.37 (2H, d, *J* 7.7, 3,5-PyH), 7.41–7.46 (4H, m, ArH), 7.54–7.63 (8H, m, ArH), 7.69 (1H, t, *J* 7.7, 4-PyH), 8.03 (4H, d, *J* 8.5, ArH), and 8.48 (2H, s, ArH). ¹³C NMR (CDCl₃): δ 41.0 (CH₂), 122.0 (3,5-PyC), 125.5, 125.8, 127.0, 127.1, 128.8, 130.0, 130.1, 131.7, 132.2, 135.6, 136.6, 137.2, 137.7 (4-PyC), and 157.9 (2,6-PyC). ESI-MS: *m/z* 676 [M + H]⁺, 698 [M + Na]⁺, 714 [M + K]⁺, and 1373 [2M + Na]⁺.

2.3. Photophysical measurements

UV–Vis absorption spectra were taken with a Perkin–Elmer lambda 16 spectrophotometer. Uncorrected emission (λ_{exc} = 348 nm) and corrected excitation (λ_{em} = 430 nm) spectra were obtained with a Perkin–Elmer LS 50 spectrofluorimeter. The fluorescence lifetimes (uncertainty ±5%) were obtained with an Edinburgh single-photon counting apparatus, in which the flash lamp was filled with D₂. Luminescence quantum yields (uncertainty ±15%) were determined using quinine sulfate in 0.5 M H₂SO₄ aqueous solution (Φ = 0.546 [12]). In order to allow comparison of emission intensities, corrections for instrumental response, inner filter effects, and phototube sensitivity were performed.

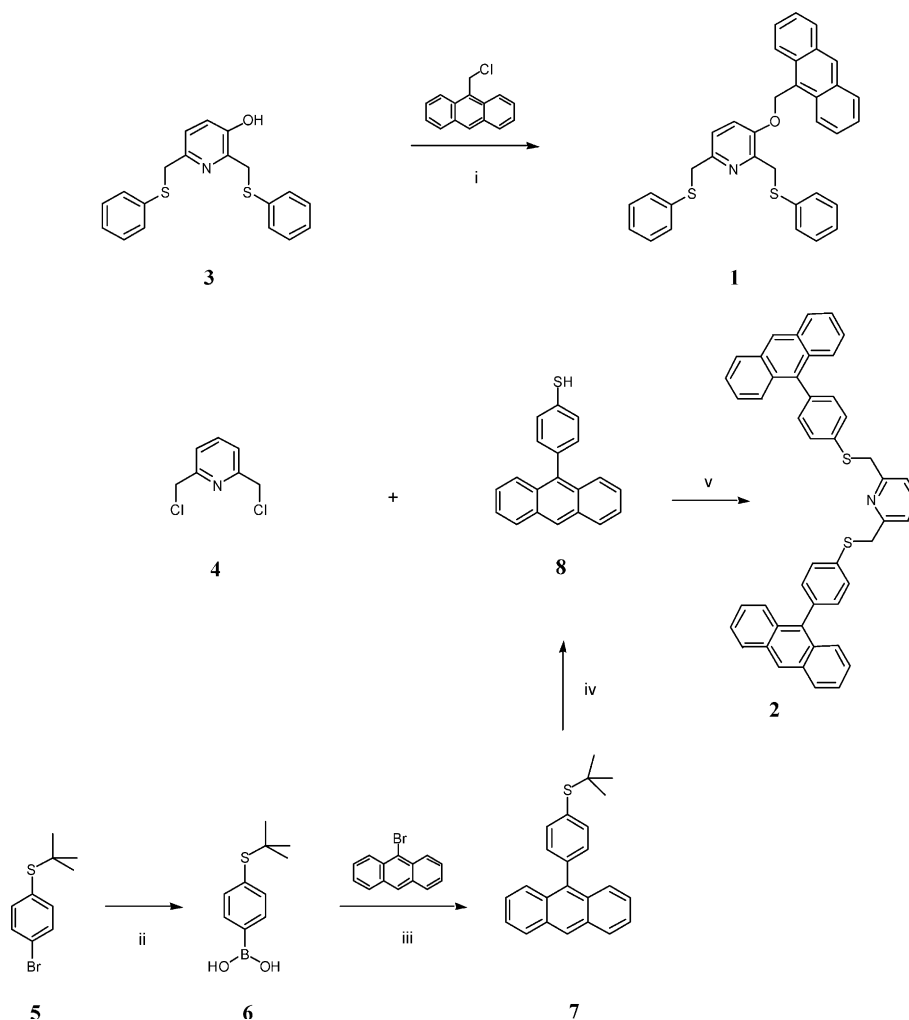
Spectrophotometric and fluorimetric titrations and data analysis were carried out as elsewhere described [13].

3. Results and discussion

3.1. Synthesis of the ligands

The fluorescent chemosensors we have developed to achieve this work incorporate a pyridyl-thioether-based binding site and the anthracene moiety as a fluorophore. The synthesis of sensor **1**, Scheme 1, was obtained from the reaction of 2,6-bis(phenylthiomethyl)-3-hydroxypyridine (**3**), prepared according to the literature procedures [10], with 9-chloromethylanthracene in the presence of K₂CO₃ using DMF as a solvent. The anthracene-based sensors **2** was successfully assembled by coupling 2,6-bis(chloromethyl)pyridine (**4**) with 9-(4-mercaptophenyl)-anthracene (**8**), Scheme 1. The starting dichloromethyl derivative **4** was prepared from the corresponding dihydroxymethyl precursor according to the reported procedure [11].

The aromatic thiol **8** was obtained by first reacting the commercially available 4-bromobenzenethiol with *tert*-butyl alcohol in the presence of perchloric acid and acetic anhydride using acetic acid as the solvent [14] to give **5** in nearly quantitative yield. Lithiation of the *tert*-butyl protected bromide (**5**) and subsequent reaction



Scheme 1. Reagents and conditions: (i) DMF, K_2CO_3 , 65 °C, 24 h; (ii) THF, *n*-BuLi, triisopropyl borate, -78 °C–RT, 20 h; (iii) C_6H_6 –EtOH– H_2O , $(\text{PPh}_3)_4\text{Pd}$, K_2CO_3 , reflux, 24 h; (iv) thioanisole, TFA, $\text{CF}_3\text{SO}_3\text{H}$, 0 °C–RT, 1 h; (v) THF, NaH, 40 °C, 24 h.

with triisopropyl borate afforded the boronic acid **6** which was coupled to 9-bromoanthracene under Suzuki cross-coupling conditions using $\text{Pd}(\text{Ph}_3)_4$ as catalyst and benzene–EtOH– H_2O as solvent system to give **7** in 92% yield. Finally, deprotection of **7** to yield the corresponding thiol **8** was achieved with triflic acid and TFA in thioanisole [15].

Purification of **8**, both by crystallisation and by chromatography, did not afford a pure product. As could be observed in the ^1H NMR and GC–MS spectra, the sample showed to contain a small impurity of 9-[4-(methylthio)phenyl]anthracene. Since all our attempts to avoid the formation of this side product or to purify **8** failed, we decided to undertake the next step of the synthesis bearing in mind that the purity of **8** was estimated, from ^1H NMR spectrum, to be higher than 95%.

Then, an appropriate excess of the thiol **8** was reacted with the dichloride **4** in the presence of NaH in THF to afford the desired compound **2** in 86% yield after chromatographic purification.

Both ligands **1** and **2** were characterised by ^1H and ^{13}C NMR, ESI mass-spectrometry, as well as elemental analysis.

3.2. Photophysical properties of the ligands

The absorption spectra of **1** and **2** (Figs. 1 and 2) in acetonitrile solutions are similar and present the typical absorption bands of anthracene derivatives. As far as **2** is concerned, it is to note that the steric interaction with the peri hydrogens typically keeps the substituent in the nine position twisted out of the plane of the anthracene ring. This precludes extensive conjugation of the phenyl ring and the anthracene π electrons in the ground state, and it explains why the absorption spectra of anthracene **1** and **2** are very similar to each other.

The fluorescence spectrum of **1** (Fig. 1) shows the typical structured band of anthracene derivatives, while the fluorescence quantum yield (0.09) and the excited state lifetime (1.6 ns) are slightly lower and shorter, respectively, than those typical of 9-methylantracene.

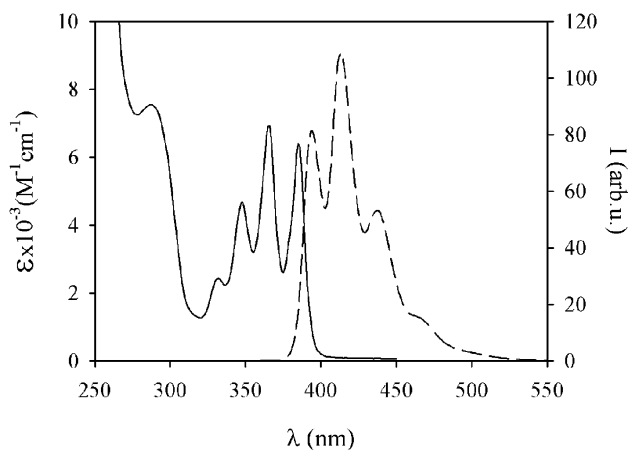


Fig. 1. Room temperature absorption (full line) and fluorescence ($\lambda_{\text{exc}} = 348$ nm, broken line) spectra of a 7.0×10^{-5} M acetonitrile solution of **1**.

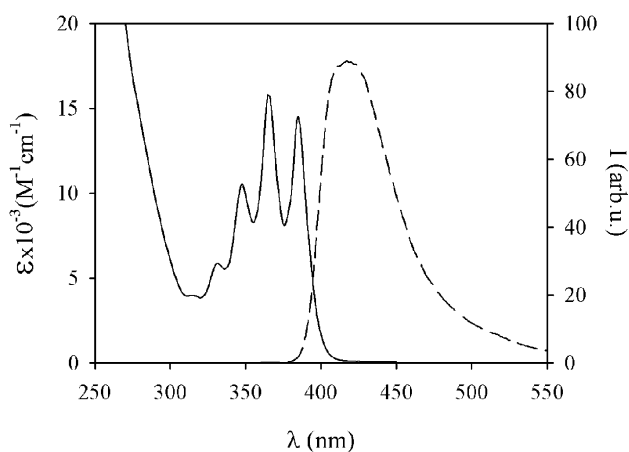


Fig. 2. Room temperature absorption (full line) and fluorescence ($\lambda_{\text{exc}} = 348$ nm, broken line) spectra of a 5.4×10^{-5} M acetonitrile solution of **2**.

The fluorescence spectrum of **2**, on the contrary, in acetonitrile does not show a clear vibrational structure, as it can be seen in Fig. 2. A more structured band can be observed in cyclohexane, quite similarly to what was observed for 9-phenylanthracene in the same solvent. The behaviour of **2** observed in acetonitrile can be most likely attributed to the rotation of the phenyl ring in the excited state to yield a geometry in which a larger delocalisation of the electronic density of the anthracene moiety is possible, as already observed, for example, in the case of 9-anthroate esters [16]. For ligand **2**, the fluorescence quantum yields remain relatively high (0.13), while the excited state lifetime (0.7) is considerably shorter than that observed for anthracene and **1**.

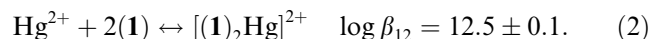
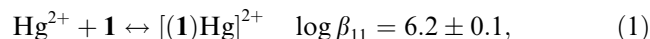
3.3. Titration experiments

In order to assess if **1** and **2** could be used as luminescent chemosensors, we performed titration experi-

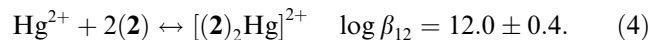
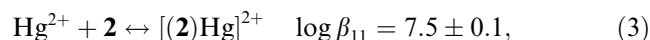
ments with different transition metal ions, and particularly with Pb^{2+} , Zn^{2+} , Cd^{2+} , Ag^+ , Cu^{2+} , and Hg^{2+} . We did not observe any change in the absorption and luminescence spectra upon addition of a 50-fold excess of Pb^{2+} , Zn^{2+} , Cd^{2+} , and Ag^+ ions to 2×10^{-5} M acetonitrile solutions of **1** and **2**. These results can certainly be attributed to the lack of complexation of these ions; otherwise at least an increase of the absorbance in the 310–330 nm region, where the complexed pyridine typically absorbs, should be observed.

On the contrary, the addition of Hg^{2+} ions leads to noticeable changes in the absorption and fluorescence spectra of the ligands. For **1**, in particular, an increase of the absorbance in the 300–350 nm and in the 260–280 nm regions can be observed, while the fluorescence band is almost completely quenched when 0.5 equivalents of metal ions are added (Fig. 3).

The spectral changes observed can be adequately interpreted if the following two equilibria are taken into account:



A very similar behaviour is shown by **2**, whose luminescence is also quenched after the addition of half an equivalent of metal ion. Again, two different equilibria can be observed, whose association constants are reported below:



The addition of Cu^{2+} ions to acetonitrile solutions of **1** and **2** leads to very similar results, i.e., an increase of the absorbance in the 300–350 nm region and a quenching

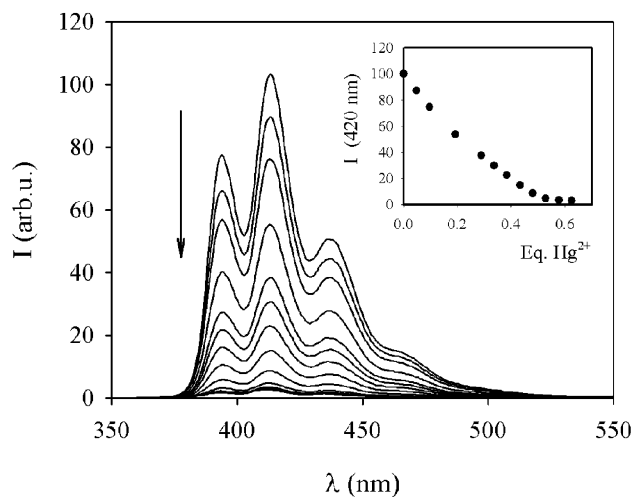
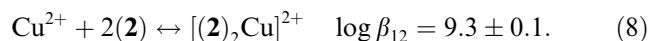
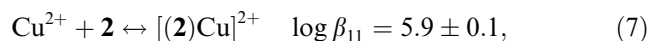
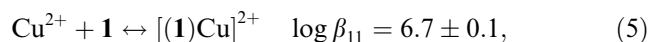


Fig. 3. Fluorescence spectra ($\lambda_{\text{exc}} = 348$ nm) of 7.0×10^{-5} M acetonitrile solution of **1** and upon addition of increasing amount of Hg^{2+} ions.

of the fluorescence band. The quenching is almost complete in the case of ligand **1**, while a 5% of residual luminescence can be observed upon addition of copper ions to ligand **2**; in both cases, however, a plateau is reached only upon addition of one equivalent of metal ion.

The observed equilibria are, also in this case, the following:



A further evidence of the formation of these complexes comes from the analysis of the ESI-MS data. When only half an equivalent of copper ion is added to a solution of **1** the peak at 1124 ($[(\mathbf{1}) + \text{Cu}]^+$) can be clearly observed, while upon addition of one equivalent also the peak at 592 ($[\mathbf{1} + \text{Cu}]^+$) clearly shows up. A very similar behaviour is shown by **2**; in this case the peaks are at 1416 ($[(\mathbf{2}) + \text{Cu}]^+$) and at 738 ($[\mathbf{1} + \text{Cu}]^+$). In the case of the mercury complexes, it was possible to observe their adducts with one anion. For example, when only half an equivalent of mercury nitrate is added to a solution of **1** the peak at 1320 ($[(\mathbf{1}) + \text{Hg} + \text{NO}_3]^+$) can be clearly observed, while upon addition of an excess of the salt also the peak at 791 ($[\mathbf{1} + \text{Hg} + \text{NO}_3]^+$) clearly shows up.

Similar results have been obtained using perchlorate or acetate salts.

In order to understand the mechanism of the fluorescence quenching upon addition of mercury and copper ions, we have also performed titration of **1** and **2** with triflic acid. An increase of the absorbance in the 300–340 nm region and a quenching of the fluorescence (both changes are more pronounced for **1** than for **2**) could again be observed. The first effect is due to the protonation of the pyridine moiety, that, as it happens for complexation, induces an increase in the absorbance in the region above 300 nm. The quenching of the luminescence can be explained in this case only assuming the occurrence of a very fast ($k_q > 10^{10} \text{ s}^{-1}$) photoinduced electron transfer process from the anthracene chromophore to the electron acceptor protonated pyridine, as schematically depicted in Fig. 4. This conclusion is supported by thermodynamic data ($E^{\circ\circ}(\text{anthracene}) = 3.21 \text{ eV}$; $E_{\text{ox}}(\text{anthracene, CH}_3\text{CN}) = 1.09 \text{ vs SCE}$ [17]; $E_{\text{red}}(\text{pyridinium ion, DMF}) = -1.2 \text{ V vs SCE}$ [18]).

A similar behaviour can be accounted for the mercury complexes, since complexation with $\text{d}^{10} \text{ Hg}^{2+}$ ions does not usually introduce low energy metal centred or charge separated excited states into the molecule, so that energy- or electron-transfer processes involving the metal ion can be ruled out. The heavy atom effect could also contribute to the non-radiative decay to the ground state; however, this effect seems to be negligible in the time scale of few picoseconds.

In the case of Cu^{2+} , that is a d^9 ion, energy- and electron-transfer processes involving the metal ion can

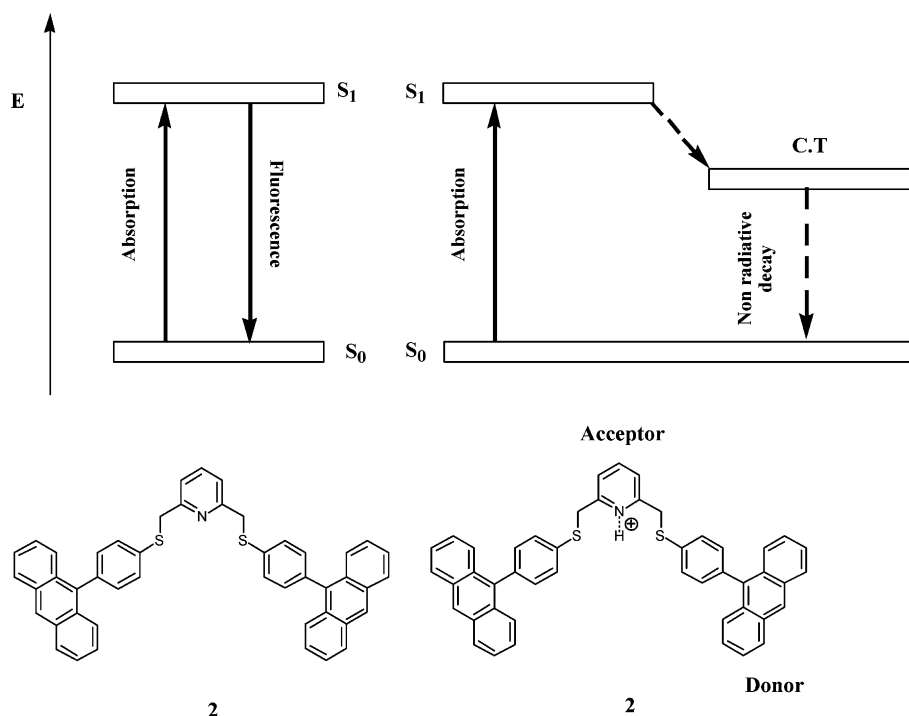


Fig. 4. Schematic representation of the energy level diagram of the protonated and unprotonated ligands.

usually occur, and their contribution in addition of the above-mentioned intraligand electron transfer process can not be ruled out.

As far as the association constants are concerned, it should be noted that the affinity of the two ligands towards Cu^{2+} and Hg^{2+} is different, but this difference is not sufficiently high to consider **1** and **2** specific chemosensors towards these analytes. However, they could find application in the so-called electronic tongues, that are instruments which include arrays of non-specific ion sensors oriented to the classification of liquid samples [19]. The concomitant use of the two ligands could therefore allow the analysis of the two metal ions at the same time.

4. Conclusions

The anthracene containing ligands **1** and **2** have a strong affinity for both Hg^{2+} and Cu^{2+} ions. For both ligands, protonation and complexation with Hg^{2+} and Cu^{2+} ions leads to dramatic changes in the photophysical properties of the anthracene chromophore, and in particular to a strong quenching of their intense luminescence. The quenching can be mainly attributed to an intraligand electron transfer process from the anthracene chromophore to the complexed pyridine. In the case of copper, a possible contribution from energy- and electron-transfer processes involving the metal ion cannot be ruled out.

The high affinity shown by **1** and **2** for Hg^{2+} and Cu^{2+} and the strong changes in the photophysical properties observed upon complexation make these compounds interesting chemosensors for these metal ions. In particular, their use in multisensory devices as the so-called electronic tongues could lead to the simultaneous detection of both these analytes in solution, a feature of particular interest for practical applications.

Acknowledgements

The authors thank MIUR, (FISR, project SAIA), and the University of Bologna (funds for Selected Topics) for funding.

References

- [1] E. Bakker, P. Bühlmann, E. Pretsch, *Chem. Rev.* 97 (1997) 3083.
- [2] P. Bühlmann, E. Pretsch, E. Bakker, *Chem. Rev.* 98 (1998) 1593.
- [3] O.S. Wolfbeis, in: A.M.V. Scheggi (Ed.), *Biomedical Optical Instrumentation and Laser-Assisted Biotechnology*, Kluwer Academic Publishers, Dordrecht, 1996, pp. 327–337.
- [4] U.E. Spichiger-Keller, *Chemical Sensors and Biosensors for Medical and Biological Application*, Wiley-VCH, Berlin, 1997.
- [5] A.W. Czarnik (Ed.), *Fluorescent Chemosensors for Ion and Molecule Recognition*, ACS Symposium Series 538, American Chemical Society, Washington, 1992.
- [6] A.P. de Silva, H.Q.N. Gunaratne, T. Gunnlaugsson, A.J.M. Huxley, C.P. McCoy, J.T. Rademacher, T.E. Rice, *Chem. Rev.* 97 (1997) 1515.
- [7] B. Valeur, I. Leray, *Coord. Chem. Rev.* 205 (2000) 3.
- [8] (a) C. Bargossi, M.C. Fiorini, M. Montalti, L. Prodi, N. Zaccheroni, *Coord. Chem. Rev.* 208 (2000) 17;
(b) L. Prodi, F. Bolletta, M. Montalti, N. Zaccheroni, *Coord. Chem. Rev.* 205 (2000) 59;
(c) M. Montalti, L. Prodi, N. Zaccheroni, in: Nalwa (Ed.), *Handbook of Photochemistry and Photobiology*, M.S.A. Abdel-Mottaleb, H.S. Nalwa Eds., American Institute of Physics, Stevenson Ranch 3 (2003) 271–317.
- [9] (a) A. Credi, L. Prodi, *Spectrochim. Acta Part A* 54 (1998) 159;
(b) M. Montalti, L. Prodi, N. Zaccheroni, G. Falini, *J. Am. Chem. Soc.* 124 (2002) 13540.
- [10] G. Chessa, L. Canovese, L. Gemelli, F. Visentin, R. Seraglia, *Tetrahedron* 57 (2001) 8875.
- [11] L. Canovese, G. Chessa, G. Marangoni, B. Pitteri, F. Visentin, P. Uguagliati, *Inorg. Chim. Acta* 186 (1991) 79.
- [12] S.R. Meech, D. Phillips, *J. Photochem.* 23 (1983) 193.
- [13] (a) L.J. Charbonnière, R. Ziessel, M. Montalti, L. Prodi, N. Zaccheroni, C. Boehme, G. Wipff, *J. Am. Chem. Soc.* 124 (2002) 7779;
(b) L. Prodi, M. Montalti, N. Zaccheroni, G. Pickaert, L. Charbonnière, R. Ziessel, *New J. Chem.* 27 (2003) 134.
- [14] S.E. Gibson, N. Guillo, A.J.P. White, D.J. Williams Soc., *J. Chem., Perkin Trans.* (1996) 2575.
- [15] B. Barlaam, T.G. Bird, C. Lambert-van der Brempt, D. Campbell, S.J. Foster, R. Maciewicz, *J. Med. Chem.* 42 (1999) 4890.
- [16] R. Shao-lin Shon, D.O. Cowan, W.W. Schmlegel, *J. Phys. Chem.* 20 (1975) 2087.
- [17] C.K. Mann, K.K. Barnes, *Electrochemical Reactions in Nonaqueous Systems*, Marcel Dekker Inc., New York, 1970.
- [18] M. Marcaccio, private communication.
- [19] A. D'Amico, C. Di Natale, R. Paolesse, *Sens. Actuators B* 28 (2000) 324.